ELSEVIER

PII: S0032-3861(96)00898-1

Polymer Vol. 38 No. 14, pp. 3645–3653, 1997

0032-3861/97/$17.00+0.00

Inhomogeneous structure of polyurethane networks based on poly(butadiene)diol: 2. Time-resolved SAXS study of the microphase separation

Ivan Krakovský*
Institute of Macromolecular Chemistry, Academy of Sciences of the Czech Republic, Heyrovský Sq.2, 162 06 Prague, Czech Republic

and Hiroshi Urakawa and Kanji Kajiwara
Faculty of Engineering and Design, Kyoto Institute of Technology, Kyoto, Sakyo-ku, Matsugasaki 606, Japan
(Received 25 October 1995; revised 26 July 1996)

The process of the microphase separation leading to an inhomogenous structure of the polyurethanes prepared from poly(butadiene)diol (PBD), 4,4′-diphenylmethane diisocyanate (MDI) and poly(oxypropylene)triol (POPT) has been investigated by synchrotron small-angle X-ray scattering (SAXS). The development of the two-phase structure of the polyurethanes, consisting of microdomains of higher electron density dispersed in the matrix of PBD chains, was revealed. When POPT is not used in the preparation, the interdomain distance does not increase with time and it corresponds to the root-mean-square end-to-end distance of the PBD chains. In the presence of POPT a distinct growth in the microdomain size and interdomain distance is observed. The scattering data are discussed in terms of the modified Percus–Yevick hard sphere model. © 1997 Elsevier Science Ltd.

(Keywords: small-angle X-ray scattering; polyurethane; poly(butadiene)diol)

INTRODUCTION

The microphase separated structure composed of hard and soft segment phases accounts for the unique properties of segmented copolymers. Therefore, information about the development of such a structure is of great interest from a practical as well as a fundamental viewpoint.

Phase-separation process in segmented polyurethanes has been studied by various methods, such as differential scanning calorimetry (d.s.c.)[1,2], Fourier transform infrared spectroscopy (*FT*i.r.)[3] or pulsed proton magnetic resonance[4]. However, all these techniques represent indirect ways to follow the process. More direct information is provided by small-angle X-ray scattering (SAXS), especially, when using high-intensity synchrotron sources of X-rays, now available. Synchrotron SAXS was used, e.g. by Li *et al.* to investigate the phase-separation process in linear segmented polyurethanes[5] based on poly(tetramethylene oxide) end-capped with poly(propylene oxide), MDI and 1,4-butanediol.

Usually, the microphase separation in block or segmented copolymers is induced by thermal quenching of the system from the homogeneous molten state. Depending on the way the system goes through phase space, two mechanisms of the phase separation may be observed in *early* stages of the process[6]: nucleation and growth (NG) mechanism or spinodal decomposition (SD). The scattering intensity in the former case should increase with time squared[7], and exponential increase with time is predicted in the latter case[8,9]. However, saturation effects soon become important at *later* times and the intensity growth is slowed down. Finally, Ostwald ripening[10], in which larger droplets of one phase grow at the expense of smaller ones, may occur. In lower minor phase fraction (less than *ca.* 30%) NG as well as SD mechanism usually lead to the particulate morphology, in commensurate phase fractions the SD mechanism is expected to give cocontinuous morphology.

However, the process of the phase separation during the formation of segmented copolymers is much more complicated than in non-reactive cases discussed above. Segmented copolymers are usually prepared by the reaction of telechelic prepolymers (molar mass of few thousands) and low-molecular weight compounds. During the reaction the average molecular weight and polydispersity of the reaction mixture increase. As a result of the chemical changes in the system the interaction between the species formed also varies and the system can cross the thermodynamic phase boundaries starting the phase separation by NG or SD mechanism. A vitrification or crystallization of one of the phases can occur at later times. The resultant morphology of the copolymer is determined by the competition between all these processes.

* To whom correspondence should be addressed. Present address: Department of Polymer Physics, Faculty of Mathematics and Physics, Charles University, V Molešovičkách Z, 18000 Prague 8, Czech Republic

Ryan and coworkers[11] used time-resolved SAXS in the study of the microphase separation process during the formation of the segmented polyurethane from α,ω-dihydroxy poly(oxyethylene-*block*-oxypropylene), MDI and 1,4-butanediol. They observed a scattered intensity growth consistent with NG mechanism. Elwell *et al.*[12] investigated the kinetics of microphase separation during the processing of the polyurethane foam from polyether polyol and MDI, in the presence of water and a surfactant. In this system, the microphase-separation process was shown to follow the spinodal decomposition kinetics.

In this paper, the formation of the microphase-separated polyurethane network prepared by the reaction of poly(butadiene) diol (PBD), 4,4′-diphenylmethane diisocyanate (MDI) and poly(oxypropylene)triol (POPT) as the crosslinking agent investigated by time-resolved synchrotron SAXS is reported. The structure of this system was revealed[13] as composed of two phases where one of the phases consists of PBD chains and the other of densely crosslinked POPT/MDI network with much higher glass transition temperature.

EXPERIMENTAL

Materials

Three polyurethane mixtures, A, B and C, were prepared from PBD, MDI and POPT. The characteristics of the starting materials are given in the previous paper[13]. The initial molar ratios of reactive groups and the weight fractions of components are given in *Table 1*. Immediately before the measurement, the reaction components were mixed intensively by an electromagnetic stirrer at 60°C. After 5 min of stirring, a small amount of the catalyst (0.001 wt% dibutyltin dilaurate) was added to the mixture which was then stirred for another 5 min. A small amount of the mixture necessary for the measurement was put into a holder with windows covered by thin mica slices. The sample thickness as defined by the distance between mica slices was *ca* 1.0 mm. All three mixtures were transparent.

Small-angle X-ray scattering

The SAXS measurements were performed with SAXES optics installed at BL-10C of the Photon Factory, Tsukuba[14]. The time-resolved SAXS measurements were started immediately after putting the reaction mixtures into the cell thermostatted at 70°C. Two-minute SAXS measurements were repeated with an appropriate time interval over a necessary period.

The scattering intensities were corrected for the parasitic scattering and the absorption of the samples.

RESULTS AND DISCUSSION

Figures 1 and *2* show the time-resolved SAXS (dependence of the scattering intensity on the magnitude of the scattering vector $q = (4\pi/\lambda)\sin(\theta/2)$, where λ and θ are the wavelength and the scattering angle, respectively) from the mixtures A and B in 10 min intervals. The intensity of both mixtures increases gradually with time approaching a final value after about 90 min. A scattering peak is progressively formed in both cases, while the position of the peak ($q_{max} \approx 0.11$ Å^{-1}) does not seem to shift with time. The intensity of the mixture B is higher than that of mixture A due to the higher content of MDI, which is the component of the highest electron density.

On the other hand, the presence of POPT (mixture C) has a strong influence on the scattering behaviour of the system as observed by SAXS as can be seen from *Figure 3*. The composition of this mixture corresponds to that of the film sample UR3 investigated in the previous paper[13] having a distinct scattering peak. The figure shows a progressive growth of the intensity which is much higher than in the case of the mixtures A and B, and the formation of the scattering peak. The position of the peak at the beginning of the measurement (*ca* 0.08 Å^{-1}) is near the position in the mixtures A and B. As time progresses it shifts towards lower values of q; however, after about 100 min it remains constant.

The position of the peak at SAXS patterns provides information about the periodic variation[15,16] of electron density characterized by a Bragg spacing D

$$D = \frac{2\pi}{q_{max}} \tag{1}$$

The values of the Bragg distance of the mixtures were determined after smoothing of the experimental scattering patterns and their time dependences are given in *Figure 4*. When POPT is not present in the reaction (mixtures A and B), no distinct change in the Bragg distance is revealed. In both cases the magnitude of the Bragg distance is about 60 Å and it is close to the root mean square end-to-end distance of the PBD chain of given molecular weight (*ca* 61 Å, see ref. 17).

In the case of the mixture C, the Bragg distance increases from about 80 Å at the beginning of the measurement to a constant value of *ca* 120 Å after about 100 min. This value corresponds well to that found for the film of the same composition (112 Å, see ref. 13). Therefore, it may be assumed that the formation of a two-phase structure with particulate morphology composed of microdomains from POPT and MDI molecules is observed. The initial increase in D reflects the increase in the interdomain distance due to the decreasing number of microdomains in the system.

The constant position of the scattering peak in the mixtures A and B would reflect the SD mechanism of the phase separation, however, the peak intensities do not grow exponentially with time. Due to a time lag between the system preparation and start of SAXS measurement it was not possible to collect time-resolved

Table 1 The initial molar ratios of reactive groups and the weight fractions of components of the reaction mixtures

Mixture	$[OH]_{PBD}$:	$[NCO]_{MDI}$:	$[OH]_{POPT}$	w_{PBD}	w_{MDI}	w_{POPT}
A	1 :	1 :	0	0.956	0.044	–
B	1 :	2 :	0	0.915	0.085	–
C	1 :	2 :	1	0.846	0.078	0.076

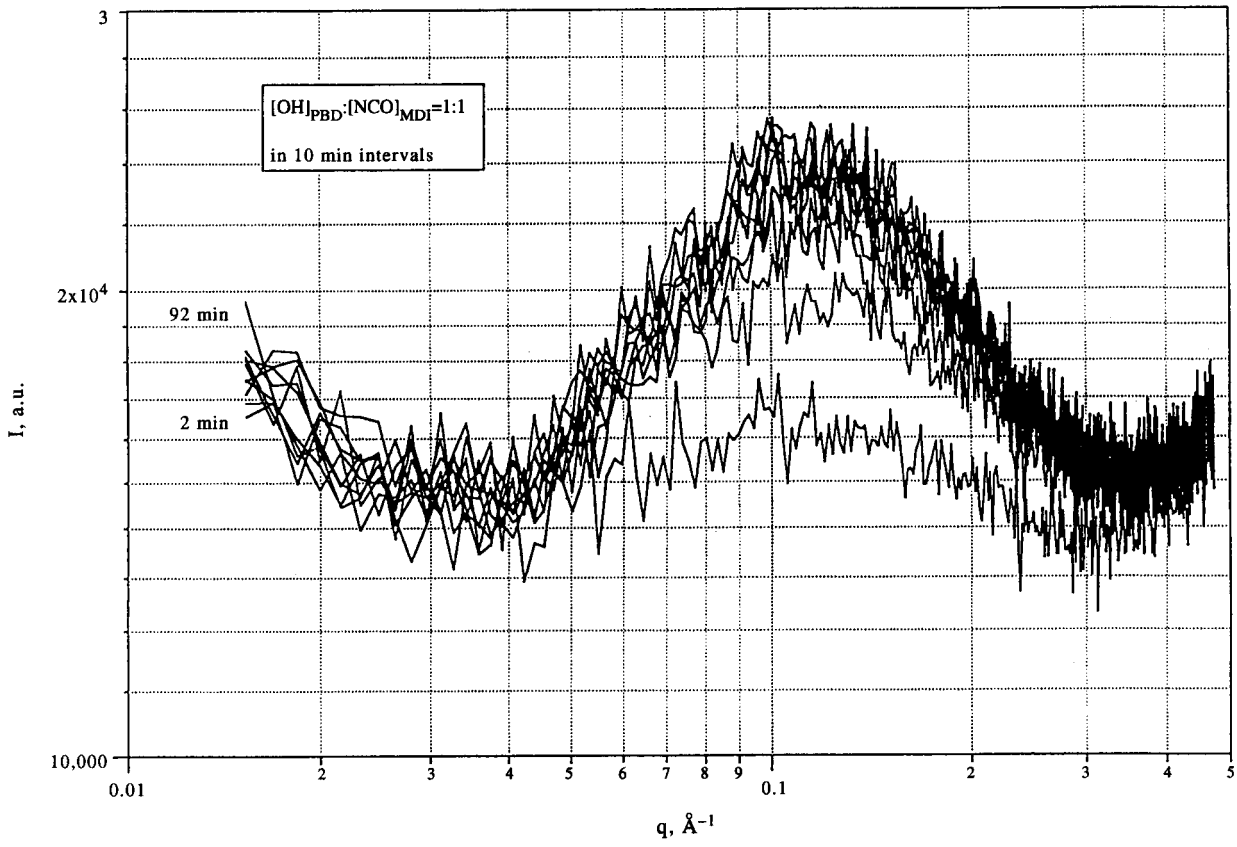

Figure 1 Time dependence of SAXS patterns (scattering intensity I in arbitrary units vs. magnitude of the scattering vector q) of the mixture A

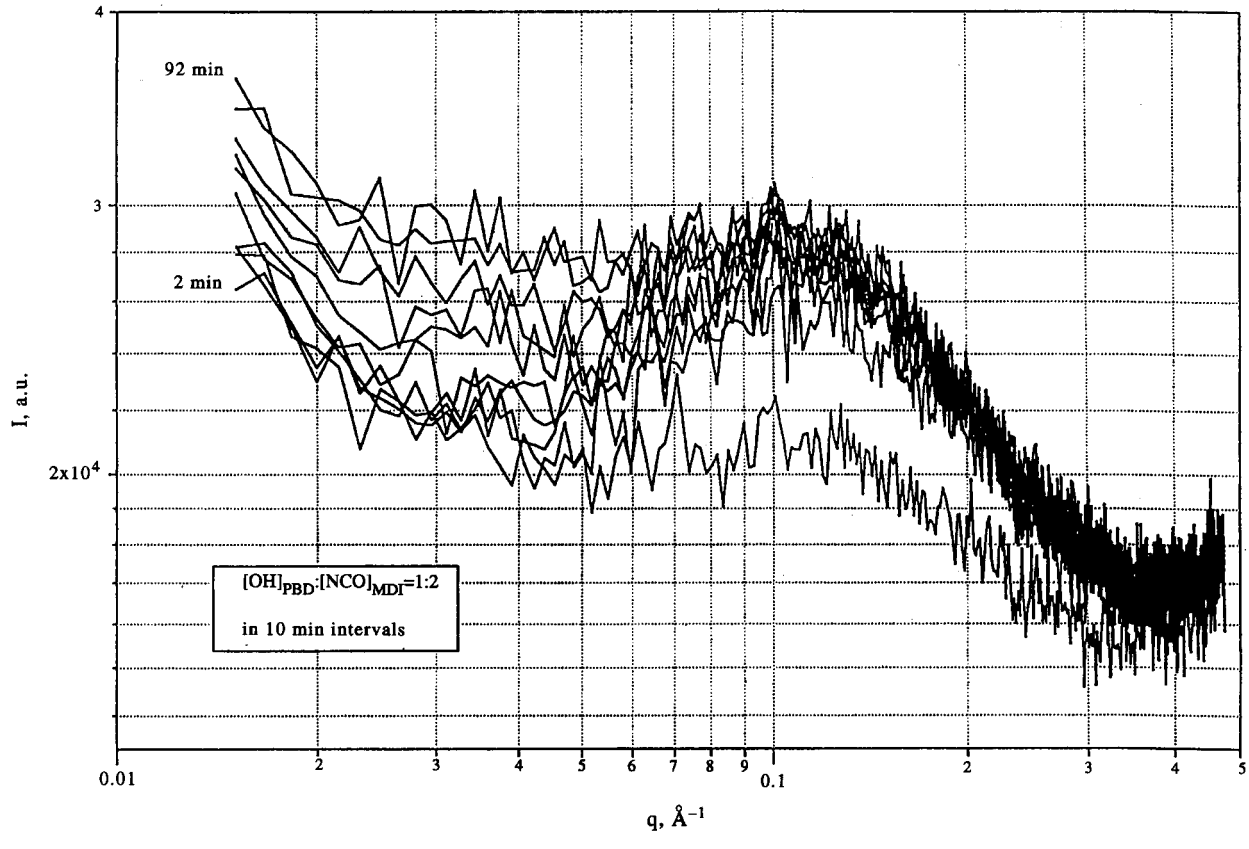

Figure 2 Time dependence of SAXS patterns of the mixture B

SAXS patterns from its very beginning; thus, only later stages of the phase-separation process were observable in the experiment.

The time dependence of the scattering intensity for various values of the scattering vector is given in *Figures 5a, b*. The intensity grows the most rapidly for $q \approx q_{max}$ when it requires the longest time to reach its final value. However, the time evolution of scattering intensity for lower q values ($q < 0.01$ Å^{-1}) seems to consist of two stages. In the first 40 min of the first stage (cf. *Figure 5b*) the growth is almost linear with time; at the second stage it is accelerated, especially in proximity of the scattering peak. A final value of the scattering intensity is reached after a long time. The process probably involves two mechanisms, however, its description by a kind of a double-relaxation equation seems to be difficult.

For higher q values $q > 0.1$ Å^{-1}, the intensity increases slowly and attains its final value earlier. The behaviour in

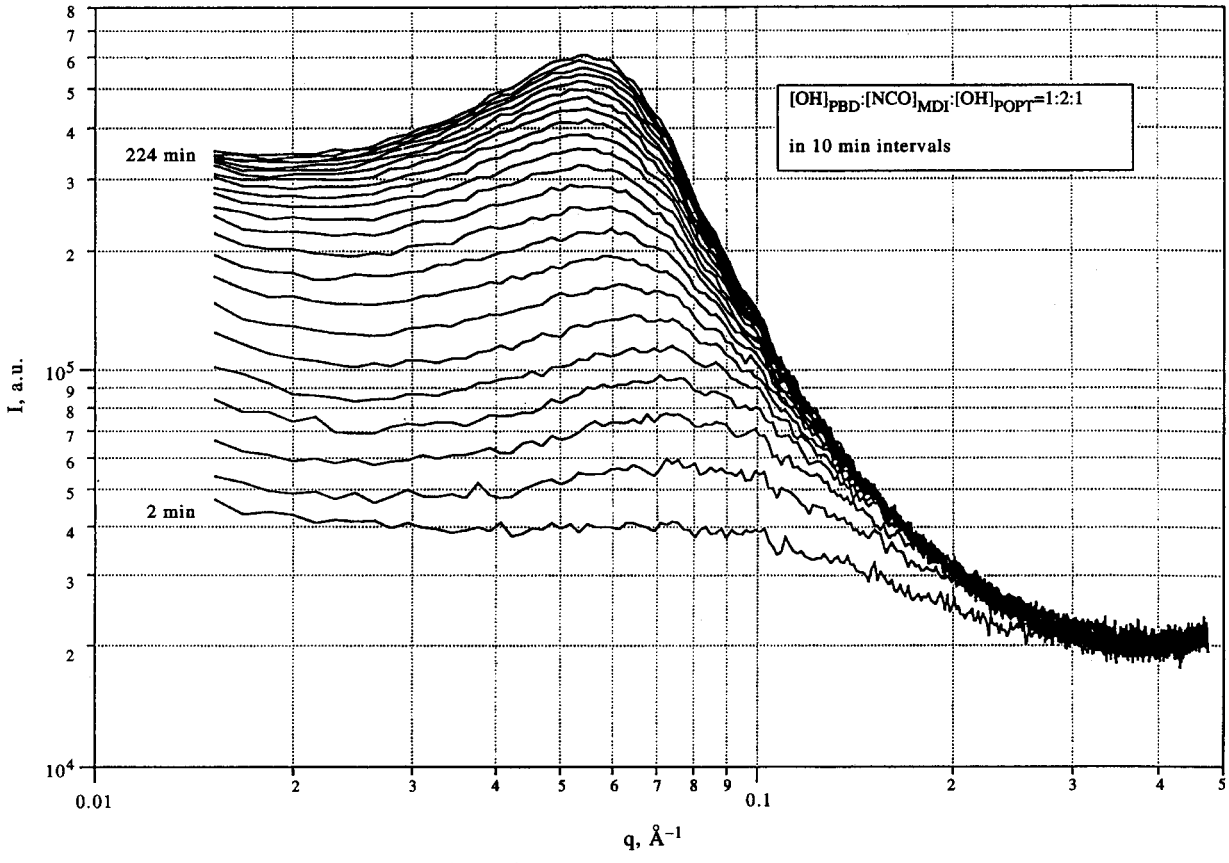

Figure 3 Time dependence of SAXS patterns of the mixture C

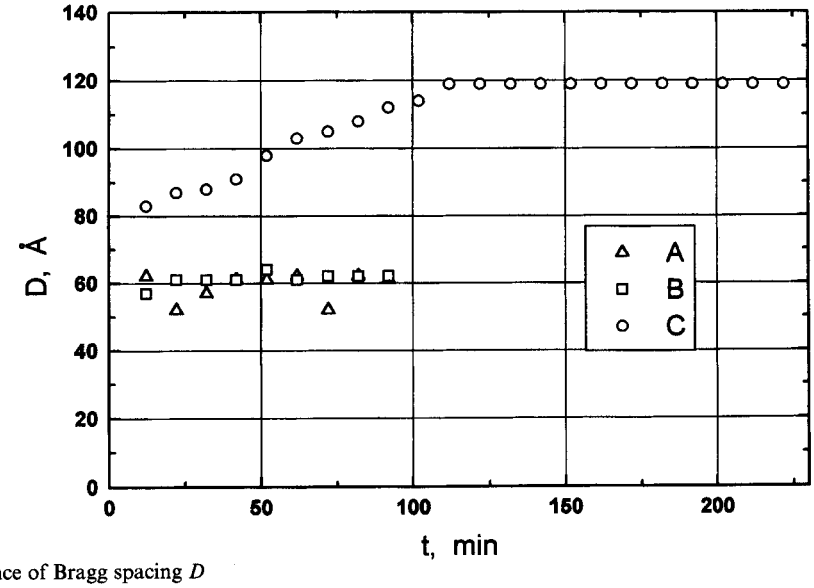

Figure 4 Time dependence of Bragg spacing D

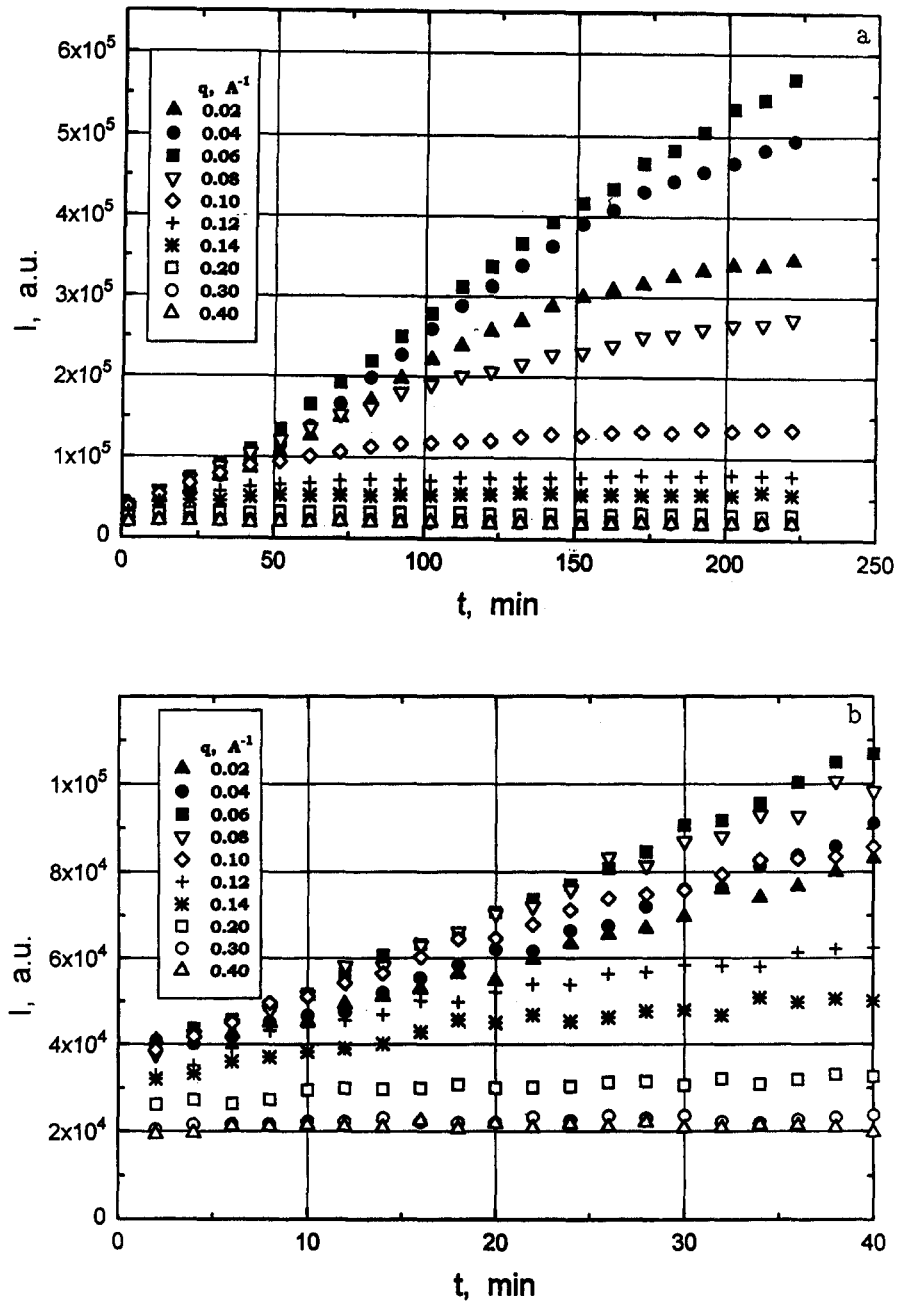

Figure 5 Time dependence of scattering intensity I for different magnitudes of scattering vector q in (a) long- and (b) short-time scale

this q region can be described by an equation of relaxation with a single-relaxation time τ

$$\frac{I(q,\infty)-I(q,t)}{I(q,\infty)-I(q,t_0)}=\exp[-t/\tau(q)] \qquad (2)$$

where $I(q,\infty)$ and $I(q,t_0)$ are the values of the intensity at the end and the beginning of the phase-separation process, respectively. The relaxation time τ decreases with increasing q (see *Figure 6*), for $q > 0.25\,\text{Å}^{-1}$ its determination becomes not reliable. The strong dependence of relaxation time on q means that the structures of different space scales aggregate together.

The integral of scattering intensity,

$$Q=\int_0^\infty q^2 I(q)\mathrm{d}q \qquad (3)$$

which is independent of the structural details of the system (scattering invariant), can serve as a relative measure of the phase separation in the system[5].

The scattering invariant Q increases continuously with time progress for all three mixtures (see *Figure 7*), indicating an increase in the degree of phase separation. The experimental values can be again fitted well by a single-relaxation equation:

$$\frac{Q(\infty)-Q(t)}{Q(\infty)-Q(t_0)}=\exp(-t/\tau_Q) \qquad (4)$$

where $Q(\infty)$ and $Q(t_0)$ are the values of Q at the end and the beginning of the phase-separation process, respectively. The corresponding values of the relaxation time τ_Q for the mixtures A, B and C are 15, 12 and 76 min, respectively. This confirms that crosslinking decreases the rate of phase separation and microdomain formation.

As it was mentioned in our previous paper (see ref. 13),

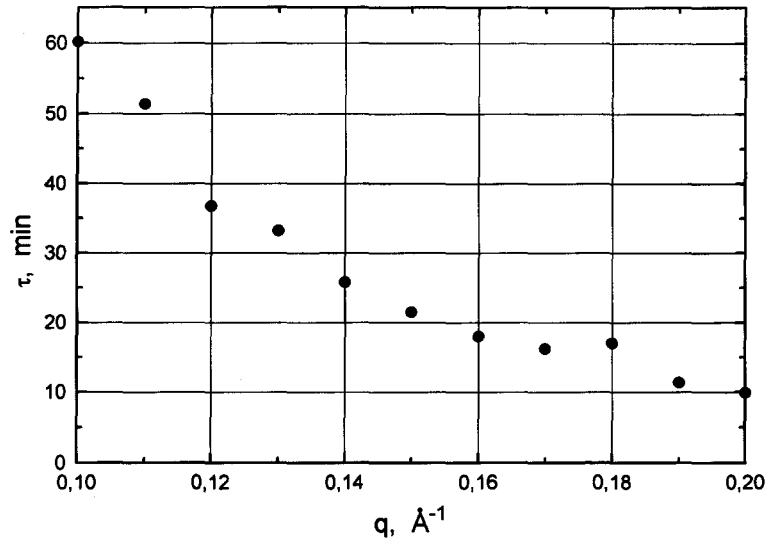

Figure 6 Dependence of relaxation time τ on magnitude of the scattering vector q

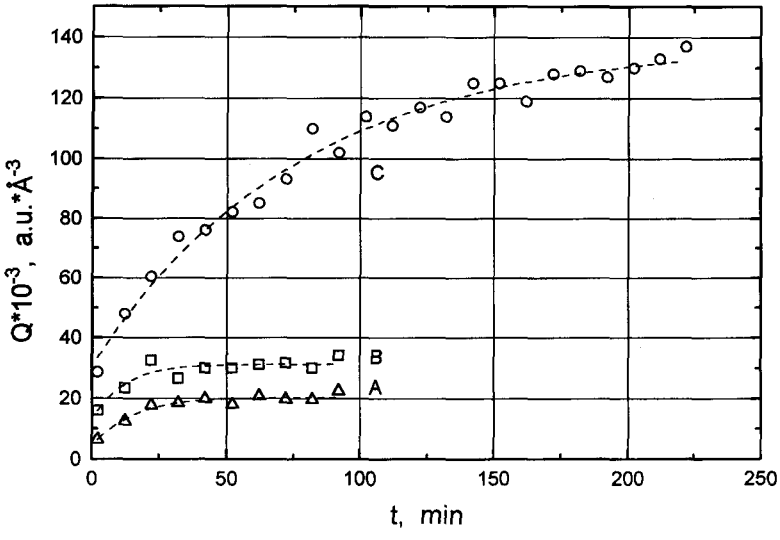

Figure 7 Time dependence of scattering invariant Q. Dashed lines represent fitting by equation (4)

the large difference in polarity of MDI and polybutadiene segments seems to be a probable cause for the phase separation in the polyurethane systems studied here. As NCO groups of MDI react with terminal hydroxy groups of PBD chains, the associates of the hydroxy groups present in pure PBD[18] serve as the probable nuclei for the phase separation. The proximity of the magnitude of Bragg distance, determined for the mixtures A and B and the root mean square end-to-end distance of the PBD chain seem to confirm this assumption.

The presence of POPT in the mixture C slows down the microdomains growth as, in this case, NCO groups of MDI can also react with terminal hydroxy groups of POPT giving rise to larger and less mobile branched molecules. These molecules diffuse more slowly inside the microdomains formed in a similar way as in the mixtures A and B. In early stages of the process, the microdomains formed must also merge with each other as the Bragg distance increases with time. However, after some time, due to increasing size and extent of the reaction the mobility of the microdomains is restricted which is reflected by constant scattering peak position. As the value of the scattering invariant still increases in later stages of the process, the microdomains grow via a diffusion of MDI and POPT molecules, still dispersed out of microdomains. In this stage the microdomains become densely crosslinked.

To obtain more detailed information about the systems, a different approach to that used usually in studies of phase separation process, was examined. The approach is based on the modified Percus–Yevick hard-sphere model incorporated in the Debye–Bueche particle scattering function to simulate the observed scattering. This model proved to be successful in the description of SAXS data from the polyurethane films (cf. ref. 13). The model consists of the microdomains specified by the particle scattering factor of the Debye–Bueche type with a correlation length a_{cor}, which are dispersed in a matrix

of different electron density. The microdomains interact by the hard-sphere interaction specified by a radius R_{HS}. The volume fraction of 'hard-spheres' in the system is v. The scattering intensities were fitted by using the equation

$$I(q, a_{cor}, R_{HS}, v) \propto P(q, a_{cor})S(q, R_{HS}, v)$$

where P is the Debye–Bueche particle scattering function

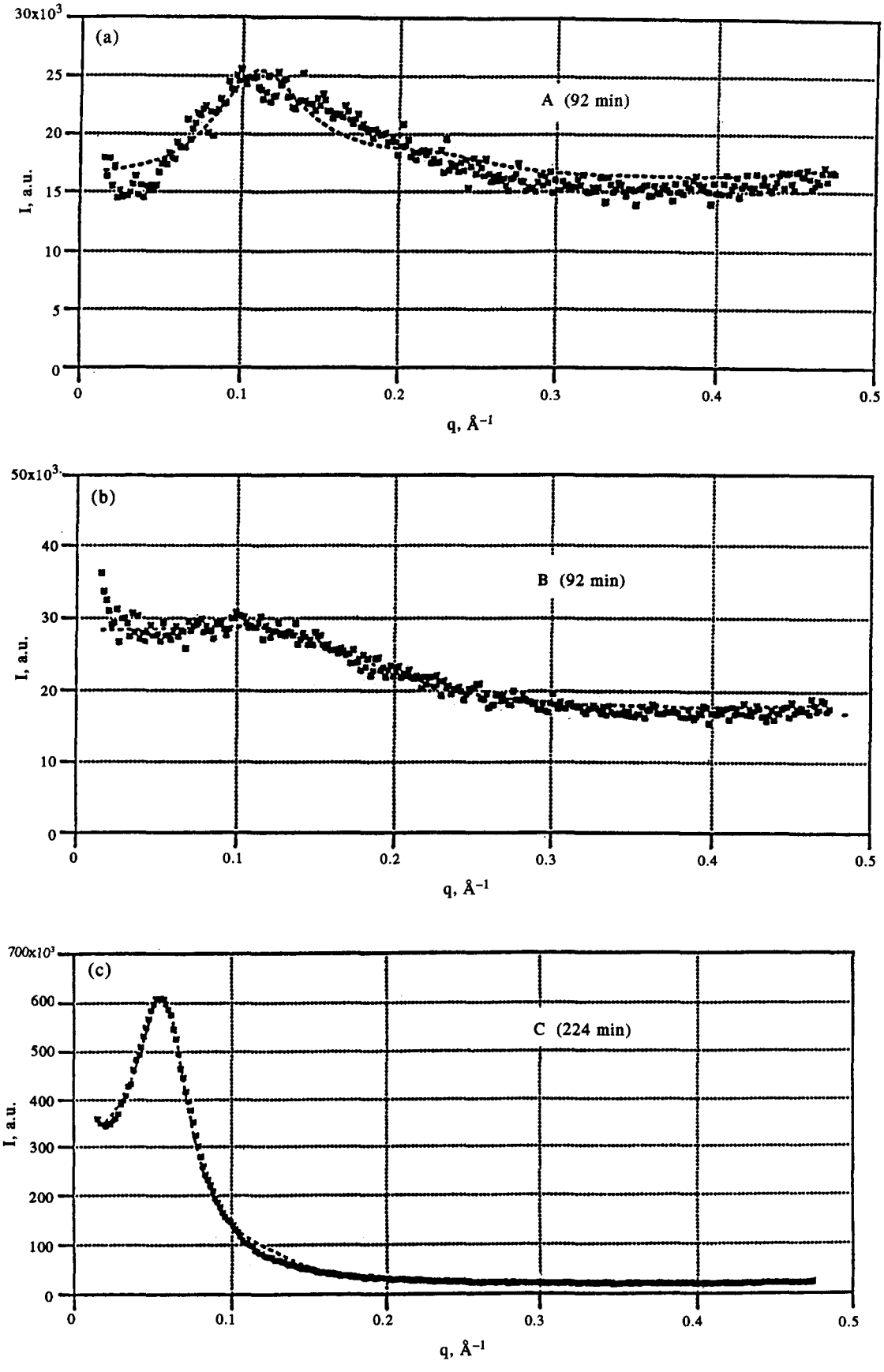

Figure 8 (a–c) Comparison of the experimental (■) and theoretical SAXS patterns calculated by using modified Percus–Yevick model (---)

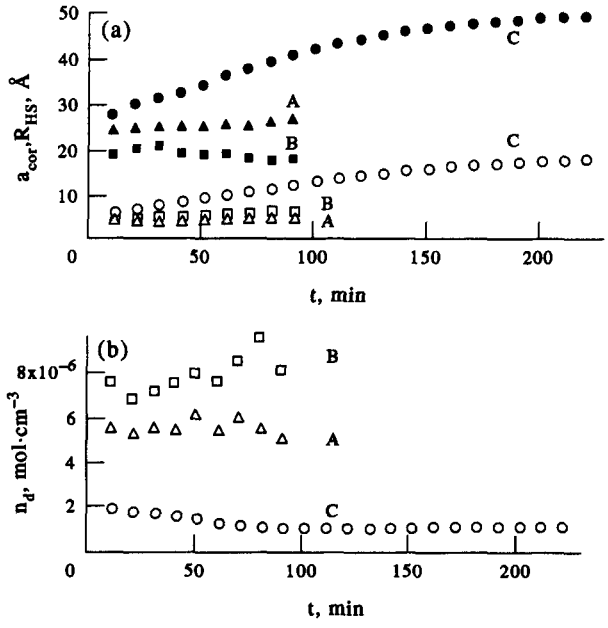

Figure 9 Time dependence of (a) correlation length a_{cor} (open symbols) and hard-sphere interaction radius R_{HS} (full symbols); and (b) microdomain concentration n_d

and S is the hard-sphere interference factor [see equations (11) and (8) in ref. 13].

Figures 8a–c give a comparison of the observed and calculated scattering patterns of mixtures for chosen times of the measurement. Background scattering was approximated by using the Vonk formula (cf. ref. 19). It can be seen that the fits are satisfactory, especially in the case of the mixtures B and C.

The dependence of the correlation length a_{cor} and hard sphere interaction radius R_{HS} on time is reported in *Figure 9a*. For the mixtures A and B, small variations in both parameters during the reaction were observed. The values of the correlation length are $a_{cor} \approx 4$ and 5 Å for the mixture A and B, respectively. The higher value of the correlation length for the mixture B is due to a higher content of MDI and consequently larger size of microdomains. The corresponding values of the interaction radius are $R_{HS} \approx 25$ and 19 Å. The value of the interaction radius for the mixture B is lower, probably due to the lower viscosity of the system as the ratio of reactive groups ($[OH]_{PBD} : [NCO]_{MDI} = 1:2$) is non-stoichiometric in this case.

In the case of the mixture C a distinct increase in a_{cor} as well as R_{HS} with time was observed. The values of both parameters at the beginning of the reaction seem to be close to those of the mixtures A and B. The increase in both parameters reflects the growth of the size of the microdomains due to the reaction between MDI and POPT. The size of the microdomains grows in the time course of reaction as the increasing amount of POPT and MDI is linked progressively to the microdomains.

From the known values of the volume fractions of hard spheres (v) and their radii (R_{HS}), the number concentration of the microdomains can be expressed as

$$n_d = \left(\frac{3v}{4\pi}\right)\frac{1}{R_{HS}^3} \qquad (5)$$

Time dependence of the number concentration of microdomains is shown in *Figure 9b*. No systematic trend of the time dependence was observed for the mixtures A and B ($n_d \approx 6 \times 10^{-6}$ mol cm^{-3} and 8×10^{-6} mol cm^{-3}, respectively).

In the case of the mixture C, the number concentration of the microdomains is much lower and further decreases with reaction time, approaching a constant value ($n_d \approx 0.8 \times 10^{-6}$ mol cm^{-3}) after about 100 min of measurement. These conclusions are consistent with the more general discussion given above.

The average number of PBD chain ends connected to one microdomain N_E via the reaction of their terminal hydroxy groups can be evaluated from the values of the number concentration of the microdomains by using the relation

$$N_E = \frac{\bar{f}_n w_{PBD} d}{\bar{M}_n n_d} \qquad (6)$$

where $\bar{f}_n$ and $\bar{M}_n$ are the average number of the hydroxy groups and the number-average molar mass of PBD chains (1.91 and 5100 g mol^{-1}, respectively; see ref. 13), w_{PBD} is the weight fraction of PBD (see *Table 1*) and d is the density of the mixture (*ca* 0.9 g cm^{-3}). The values of N_E in the mixtures A, B and C, estimated in this manner are *ca* 53, 40 and 360, respectively.

CONCLUDING REMARKS

The process of the formation of microphase separated polyurethanes from the reaction mixtures of PBD, MDI and POPT has been investigated using SAXS. The time-resolved SAXS intensities can be fitted well by use of the Percus–Yevick hard-sphere model incorporated in the Debye–Bueche particle scattering function. The model is shown to provide information about the formation of microdomains which are dispersed in the matrix of PBD chains. This information is consistent with the conclusions deduced from more general analysis.

When POPT is not present in the reaction, linear segmented polyurethane is formed. The interdomain distance remains at about 60 Å in terms of Bragg spacing, and is almost constant with reaction time. The interdomain distance is independent of the content of MDI in the system, and is close to the root-mean-square end-to-end distance of the PBD chains. Microdomains consistent of aggregates of about ten MDI molecules reacted with terminal hydroxy groups of PBD and they are joined by means of PBD chains. The microdomains have to be formed relatively quickly in early stages of the reaction, as no distinct change in their number concentration with time was found.

POPT in the reaction mixture significantly promotes the growth of microdomains with respect to their size. Here a growth and shift of the distinct scattering peak with reaction time was observed, however, the system needs longer time to attain a final state. The microphase separation process consists of two stages. In the first one, the microdomains of mutually linked POPT and MDI molecules grow via a diffusion and reaction of these molecules. The microdomains also merge each with the other until their mobility is restricted due to size and degree of crosslinking. In the later stage the microdomains grow only by the diffusion of the POPT and MDI molecules still present in the surrounding mixture. As the diffusion is accompanied by the chemical reaction between MDI and POPT, in which branched and

crosslinked species are being formed, microdomains require much longer time for their growth.

ACKNOWLEDGEMENTS

The first author is thankful to Japan Society for the Promotion of Science which provided the opportunity for his stay in Japan. The work was performed under the approval of the Photon Factory Advisory Committee (Proposal No. 93G247).

REFERENCES

1. Wilkes, G. L. and Wildnauer, R., *J. Appl. Phys.*, 1975, **46**, 4148.
2. Kwei, T. K., *J. Appl. Polym. Sci.*, 1982, **27**, 2891.
3. Lee, H. S., Wang, Y. K., MacKnight, W. J. and Hsu, S. L., *Macromolecules*, 1988, **21**, 270.
4. Assink, R. A. and Wilkes, G. L., *J. Appl. Polym. Sci.*, 1981, **26**, 3689.
5. Chu, B., Gao, T., Li, Y., Wang, J., Desper, C. R. and Byrne, C. A., *Macromolecules*, 1992, **25**, 5724.
6. Olabisi, O., Robeson, L. M. and Shaw, M. T., *Polymer–Polymer Miscibility*. Academic Press, New York, 1979.
7. Lipatov, Y. S., Grigoryeva, O. P., Kovernick, G. P., Shilov, V. V. and Sergyeva, L. M., *Macromol. Chem.*, 1985, **186**, 1401.
8. Cahn, J. W., *J. Chem. Phys.*, 1965, **42**, 93.
9. Hashimoto, T., *Macromolecules*, 1987, **20**, 465.
10. Bloor, D., Brook, R. J., Flemings, M. C. and Mahajan, S. ed., *The Encyclopedia of Advanced Materials*, Vol. 3, Elsevier, 1994.
11. Ryan, A. J., Willkomm, W. R., Bergstrom, T. B., Macosko, C. W., Koberstein, J. T., Yu, C. C. and Russell, T. P., *Macromolecules*, 1991, **24**, 2883.
12. Elwell, M. J., Mortimer, S., Ryan, A. J., *Macromolecules*, 1994, **27**, 5428.
13. Krakovský, I., Bubeníková, Z., Urakawa, H. and Kajiwara, K., *Polymer*, 1997, **38**, 3637.
14. Ueki, T., Hiragi, Y., Izumi, Y., Tagawa, H., Kataoka, M., Muroga, Y., Matsushita, T. and Amemiya, Y., *Photon Factory Activity Report* **1**, V7, V29, V170, 1983.
15. Guinier, A. and Fournet, G., *Small-angle Scattering of X-rays*. Wiley, New York, 1955.
16. Glatter, O. and Kratky, O. ed., *Small-angle X-ray Scattering*. Academic Press, London, 1982.
17. Krakovský, I., Pleštil, J., Ilavský, M. and Dušek, K., *Polymer*, 1993, **34**, 3437.
18. Ghafari, M. E. and Pham, Q. T., *Makromol. Chem.*, 1983, **184**, 1669.
19. Vonk, C. G., *J. Appl. Crystallogr.* 1973, **6**, 81.